

# Exploring the Electronic and Optical Properties of $\text{Cu}(\text{In},\text{Ga})\text{Se}_2$

Rongzhen Chen

Supervisor: Clas Persson

Department of Materials Science and Engineering  
Royal Institute of Technology, Stockholm SE-10044, Sweden

06-March-2015



# Outline

1 Background

2 Motivation

3 Computational methods

4 Results

- Parameterization of energy bands for CIGS
- Dielectric function for  $\text{CuIn}_{0.5}\text{Ga}_{0.5}\text{Se}_2$

5 Summary

6 Future perspectives

7 Acknowledgements

1 Background

2 Motivation

3 Computational methods

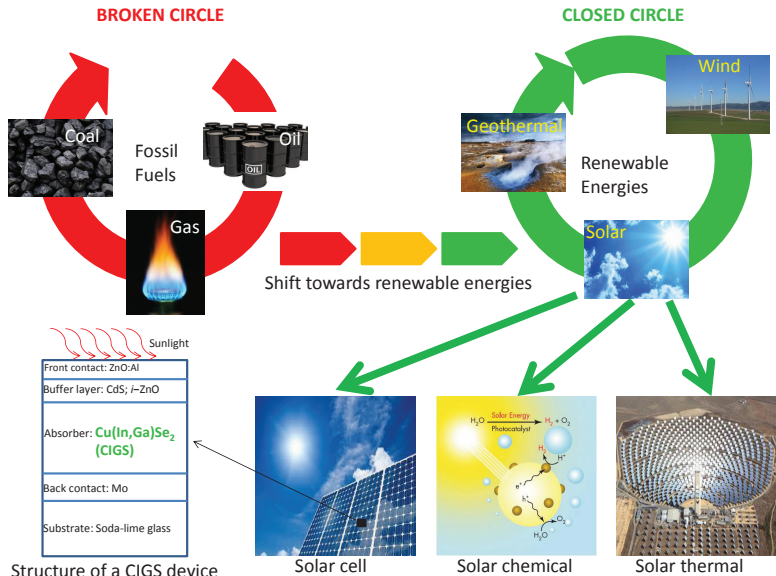
4 Results

5 Summary

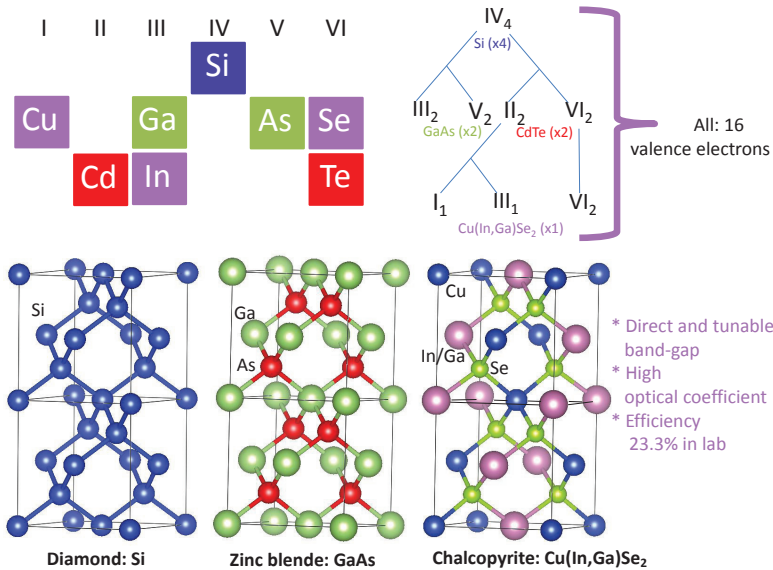
6 Future perspectives

7 Acknowledgements

# Which field and material am I working on?



# Why Cu(In,Ga)Se<sub>2</sub>?



1 Background

2 Motivation

3 Computational methods

4 Results

5 Summary

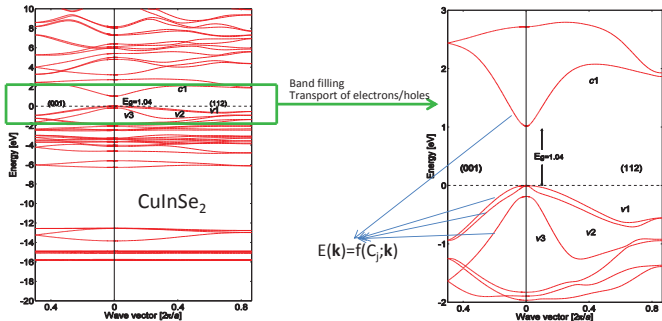
6 Future perspectives

7 Acknowledgements

# Which aspects of Cu(In,Ga)Se<sub>2</sub> have I been working on?

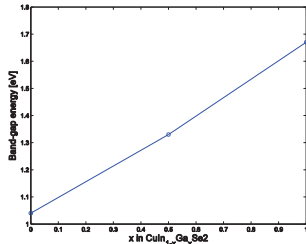
- Energy bands of CuInSe<sub>2</sub>, CuIn<sub>0.5</sub>Ga<sub>0.5</sub>Se<sub>2</sub>, and CuGaSe<sub>2</sub> are calculated by means of theoretical calculations. Parameterization of the lowest conduction (CB) and the three uppermost valence bands (VBs) are explored based on the calculated energy bands. Carrier concentration, Fermi level, and many other aspects are analyzed based on the parameterization.
- Optical properties of CuIn<sub>0.5</sub>Ga<sub>0.5</sub>Se<sub>2</sub> are explored by means of theoretical calculations.

# Motivation for the parameterization



$c1$ : the lowest conduction band (CB)  
 $v1$ : the topmost valence band (VB)

Commercially interesting:  $\text{CuIn}_{0.7}\text{Ga}_{0.3}\text{Se}_2$ ,  
 $\text{CuIn}_{0.5}\text{Ga}_{0.5}\text{Se}_2$  indicates how CIGS behaves  
when alloying In and Ga.



# Motivation for calculation of optical properties

- Help experimentalists to understand the dielectric function spectrum.
- Understand details in the optical transition for these types of materials.

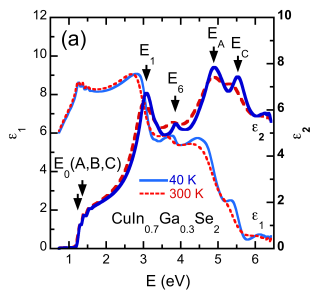


Figure : The real ( $\epsilon_1$ ) and imaginary ( $\epsilon_2$ ) part of dielectric function spectra.

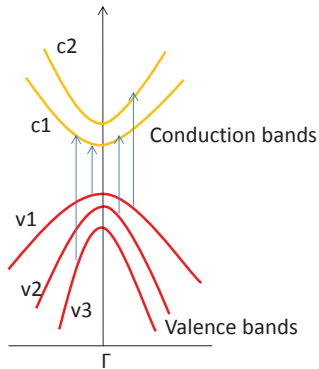


Figure : Energy bands.

- 1 Background
- 2 Motivation
- 3 Computational methods
- 4 Results
- 5 Summary
- 6 Future perspectives
- 7 Acknowledgements

# Density functional theory (DFT)

- The first theorem states that the external potential  $V_{ext}(\mathbf{r})$  is determined uniquely for any many-electron system by the ground-state electron density  $\rho$ .
- The second theorem states that there is a universal functional  $F[\rho]$  for the total energy in the terms of the electron density  $\rho$  with any external potential  $V_{ext}(\mathbf{r})$ , and the exact ground-state density is obtained when the ground state total energy functional reaches its minimal value, that is,  $E[\rho'] > E[\rho]$ . Here,  $\rho$  is the exact ground-state density.

# Kohn-Sham (KS) Equation

This problem in DFT is solved by KS equation:

$$\begin{aligned} E_{total}[\rho] &= T[\rho] + V_{int}[\rho] + V_{ext}[\rho] \\ &= T_0[\rho] + V_H[\rho] + V_{ext}[\rho] + \underbrace{(T[\rho] - T_0[\rho])}_{(V_{int}[\rho] - V_H[\rho])} \quad (1) \\ &= T_0[\rho] + V_H[\rho] + V_{ext}[\rho] + E_{xc}[\rho]. \end{aligned}$$

The KS equation in  $\mathbf{k}$ -space is derived as

$$\left( -\frac{\nabla^2}{2} + V^{KS}(\mathbf{r}) \right) \Psi_{i,k}^{KS}(\mathbf{r}) = \epsilon_{i,k}^{KS} \Psi_{i,k}^{KS}(\mathbf{r}). \quad (2)$$

The  $V^{KS}(\mathbf{r})$  is given as

$$\begin{aligned} V^{KS}(\mathbf{r}) &= V_{ext}(\mathbf{r}) + \int d\mathbf{r}' \frac{\rho(\mathbf{r}')}{|\mathbf{r} - \mathbf{r}'|} + \frac{\delta E_{xc}}{\delta \rho(\mathbf{r})} \\ &= V_{ext}(\mathbf{r}) + \int d\mathbf{r}' \frac{\rho(\mathbf{r}')}{|\mathbf{r} - \mathbf{r}'|} + V_{xc}(\mathbf{r}). \end{aligned} \quad (3)$$

# Full-potential linearised augmented-plane wave (FPLAPW)

Unit cell is divided into two regions: one is sphere region called muffin tin (MT) region, which is defined by the center of atom, but non-overlap each sphere; the remaining region is called interstitial ( $I$ ) region.

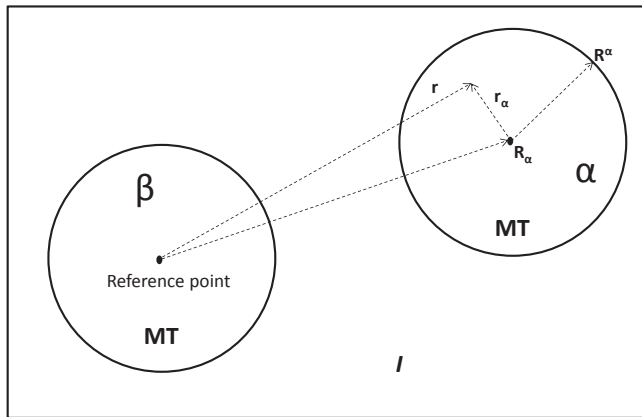


Figure : Partition of the unit cell.

The KS wavefunction can be expanded by a set of basis functions

$$\Psi_{i,\mathbf{k}}^{KS}(\mathbf{r}) = \sum_{\mathbf{G}}^{N_G} C_{i,\mathbf{k}+\mathbf{G}} \phi_{\mathbf{k}+\mathbf{G}}^{LAPW}(\mathbf{r}). \quad (4)$$

Here

$$\phi_{\mathbf{k}+\mathbf{G}}^{LAPW}(\mathbf{r}) = \begin{cases} \frac{1}{\sqrt{\Omega}} e^{i(\mathbf{k}+\mathbf{G})\mathbf{r}} & \text{if } \mathbf{r} \in I \\ \sum_{\alpha} \sum_{\ell m} f_{\ell m}(r_{\alpha}, \mathbf{k} + \mathbf{G}, \epsilon_{\ell, \alpha}) Y_{\ell m}(\hat{\mathbf{r}}_{\alpha}) & \text{if } r_{\alpha} \in MT. \end{cases} \quad (5)$$

The potential in the FPLAPW method is also divided into two regions, the MT region and the  $I$  region.

$$V(\mathbf{r}) = \begin{cases} \sum_{\mathbf{G}} V_{\mathbf{G}} e^{i\mathbf{G}\mathbf{r}} & \text{if } \mathbf{r} \in I \\ \sum_{\ell m} V_{\ell m}^{\alpha}(r_{\alpha}) Y_{\ell m}(\hat{\mathbf{r}}_{\alpha}) & \text{if } r_{\alpha} \in MT. \end{cases} \quad (6)$$

Here,  $V_{\mathbf{G}}$  and  $V_{\ell m}^{\alpha}(r_{\alpha})$  can be decided by electron density.

# The process for solving KS equation

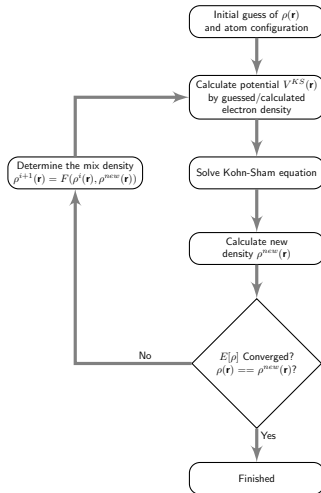


Figure : Flow chart of the  $(i + 1)$ :th iteration for solving KS equation.

1 Background

2 Motivation

3 Computational methods

4 Results

- Parameterization of energy bands for CIGS
- Dielectric function for  $\text{CuIn}_{0.5}\text{Ga}_{0.5}\text{Se}_2$

5 Summary

6 Future perspectives

7 Acknowledgements

## Result 1: Parabolic band approximation (pba)

The parabolic approximation of ellipsoidal energy bands is expressed

$$E_j^{pb}(\mathbf{k}) = E_j(\mathbf{0}) \pm \left[ \frac{\tilde{\mathbf{k}}_x^2 + \tilde{\mathbf{k}}_y^2}{m_j^\perp} + \frac{\tilde{\mathbf{k}}_z^2}{m_j^\parallel} \right] \quad (7)$$

$$\tilde{\mathbf{k}}_\alpha^2 = \frac{\hbar^2 \mathbf{k}_\alpha^2}{2e}, \text{ where } \alpha = x, y, \text{ and } z.$$

It is valid in the very vicinity of the  $\Gamma$ -point. However, away from the  $\Gamma$ -point, the parabolic approximation fails to describe the energy dispersion for the CIGS.

# Result 1: Full band parameterization (fbp)

$$\begin{aligned}
 E_j(\mathbf{k}) = & E_j^{pb}(\mathbf{k}) + E_j^0 + \Delta_{j,1} \left( \delta_{j,1}^2 \left( \frac{\tilde{\mathbf{k}}_x^4 + \tilde{\mathbf{k}}_y^4}{m_0^2} \right) + \delta_{j,2}^2 \left( \frac{\tilde{\mathbf{k}}_x^2 \tilde{\mathbf{k}}_y^2}{m_0^2} \right) + 1 \right)^{1/2} \\
 & + \Delta_{j,2} \left( \delta_{j,3}^3 \left( \frac{\tilde{\mathbf{k}}_x^6 + \tilde{\mathbf{k}}_y^6}{m_0^3} \right) + \delta_{j,4}^3 \left( \frac{\tilde{\mathbf{k}}_x^2 \tilde{\mathbf{k}}_y^4 + \tilde{\mathbf{k}}_x^4 \tilde{\mathbf{k}}_y^2}{m_0^3} \right) + 1 \right)^{1/3} \\
 & + \Delta_{j,3} \left( \delta_{j,5}^2 \left( \frac{\tilde{\mathbf{k}}_z^4}{m_0^2} \right) + 1 \right)^{1/2} + \Delta_{j,4} \left( \delta_{j,6}^3 \left( \frac{\tilde{\mathbf{k}}_z^6}{m_0^3} \right) + 1 \right)^{1/3} \\
 & + \Delta_{j,5} \left( \delta_{j,7}^2 \left( \frac{\tilde{\mathbf{k}}_x^2 \tilde{\mathbf{k}}_z^2 + \tilde{\mathbf{k}}_y^2 \tilde{\mathbf{k}}_z^2}{m_0^2} \right) + 1 \right)^{1/2} \\
 & + \Delta_{j,6} \left( \delta_{j,8}^3 \left( \frac{\tilde{\mathbf{k}}_x^4 \tilde{\mathbf{k}}_z^2 + \tilde{\mathbf{k}}_y^4 \tilde{\mathbf{k}}_z^2}{m_0^3} \right) + \delta_{j,9}^3 \left( \frac{\tilde{\mathbf{k}}_x^2 \tilde{\mathbf{k}}_z^4 + \tilde{\mathbf{k}}_y^2 \tilde{\mathbf{k}}_z^4}{m_0^3} \right) + \delta_{j,10}^3 \left( \frac{\tilde{\mathbf{k}}_x^2 \tilde{\mathbf{k}}_y^2 \tilde{\mathbf{k}}_z^2}{m_0^3} \right) + 1 \right)^{1/3}
 \end{aligned} \tag{8}$$

# Result 1: Parameterization of band structure for CIGS

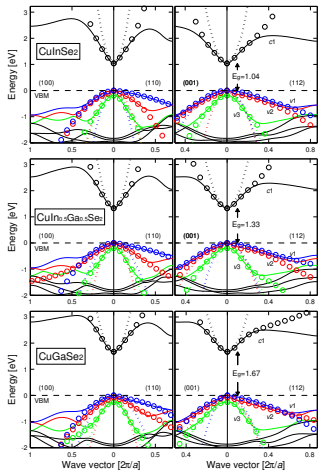


**Figure :** Electronic band structure along four directions. The circles are the results of the fbp, and the dotted lines represent the pba.

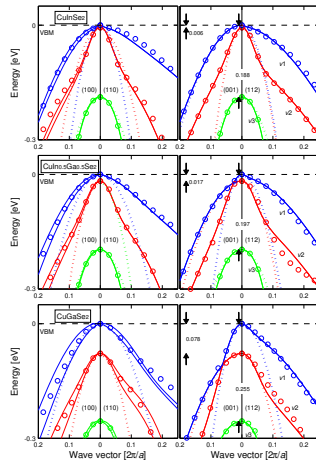


**Figure :** Close-up of right figure.

# Result 1: Non-parabolicity of the energy bands

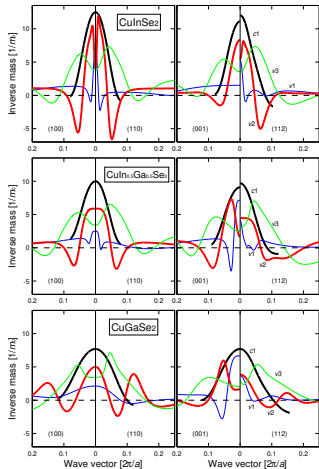


**Figure :** Inverse of the effective electron and hole masses in the four symmetry directions for the CuIn<sub>1-x</sub>Ga<sub>x</sub>Se<sub>2</sub> ( $x = 0, 0.5$ , and  $1$ ).

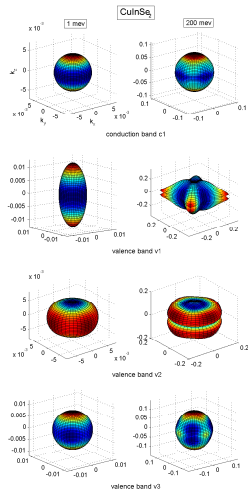


**Figure :** Constant energy surfaces for the lowest CB and three uppermost VBs in CuInSe<sub>2</sub>.

# Result 1: Density-of-states (DOS)

In the case of the pba, the density-of-states can be written as

$$g_j^{pba}(E) = \frac{1}{2\pi^2} \left( \frac{2m_j^{DOS}}{\hbar^2} \right)^{3/2} \sqrt{|E - E_j(\mathbf{0})|}. \quad (9)$$

Here, the DOS mass  $m_j^{DOS}$  is equal to  $(m_j^\perp m_j^\perp m_j^{\parallel})^{1/3}$ , which represents the extent of filling the specific band with free carriers to certain energy. In order to take advantage of the simple **Eq. 9** for the non-parabolic energy bands, the energy-dependent DOS mass ( $m_{v/c}^{DOS}$ ), which contains the non-parabolicity and anisotropy of the band dispersion, is defined as

$$g_{v/c}(E) = \sum_j g_j(E) = \frac{1}{2\pi^2} \left( \frac{2m_{v/c}^{DOS}(E)}{\hbar^2} \right)^{3/2} \sqrt{|E - E_{v1/c1}(\mathbf{0})|}. \quad (10)$$

# Result 1: Density-of-states (DOS) and DOS mass

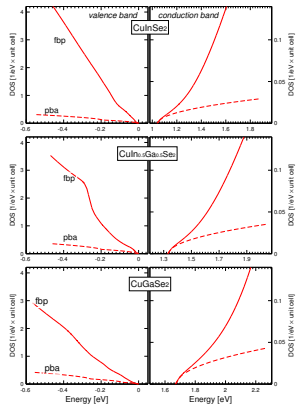


**Figure :** Total density-of-states of the VBs and CB. The solid lines show the results based on the fbp, and the dashed lines represent the results based on the pba.

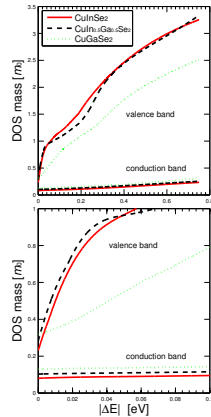


**Figure :** The DOS mass  $m_{v/c}^{DOS}$  is calculated from Eq. 10.

# Result 1: Band-gap, Fermi energy and intrinsic carrier concentration

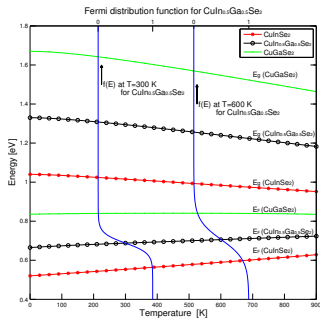


**Figure :** Band-gap energy and Fermi energy for  $1 \leq T \leq 900\text{ K}$  of intrinsic  $\text{CuInSe}_2$ ,  $\text{CuIn}_{0.5}\text{Ga}_{0.5}\text{Se}_2$ , and  $\text{CuGaSe}_2$ , determined from the fbp. The Fermi distribution  $f(E)$  of  $\text{CuIn}_{0.5}\text{Ga}_{0.5}\text{Se}_2$  is presented for  $T = 300\text{ K}$  and  $600\text{ K}$ .

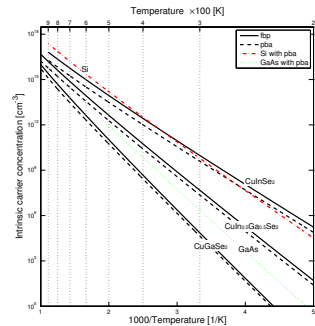


**Figure :** Intrinsic carrier concentration as function of temperature. For comparison, the theoretical results for GaAs and Si using the pba are given.

# Result 1: Carrier concentration in *p*-type for CIGS

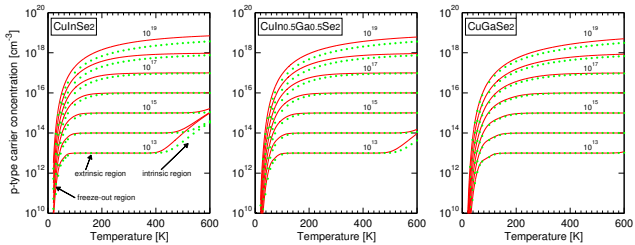


**Figure :** Free carrier concentration as function of the temperature in *p*-type for CuInSe<sub>2</sub>, CuIn<sub>0.5</sub>Ga<sub>0.5</sub>Se<sub>2</sub>, and CuGaSe<sub>2</sub>. The effective doping concentration  $N_A = 10^{13}, 10^{14}, 10^{15}, \dots$ , and  $10^{19}$  acceptors  $\text{cm}^{-3}$  are considered. Solid and dotted lines represents the fbp and the pba, respectively.

## Result 2: Dielectric function for $\text{CuIn}_{0.5}\text{Ga}_{0.5}\text{Se}_2$

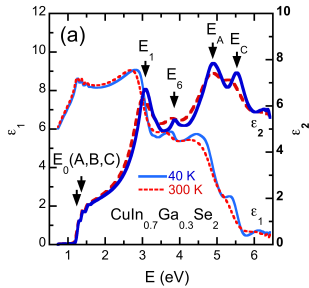


**Figure :** The real ( $\epsilon_1$ ) and imaginary ( $\epsilon_2$ ) part of dielectric function spectra for  $\text{CuIn}_{0.7}\text{Ga}_{0.3}\text{Se}_2$  at 40 K (solid blue line) and 300 K (dashed red lines). Four prominent CP features are shown.

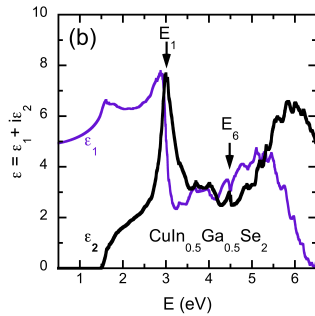


**Figure :** The dielectric function spectra for  $\text{CuIn}_{0.5}\text{Ga}_{0.5}\text{Se}_2$  calculated by FPLAPW method at 0 K. The major CP features are identified.

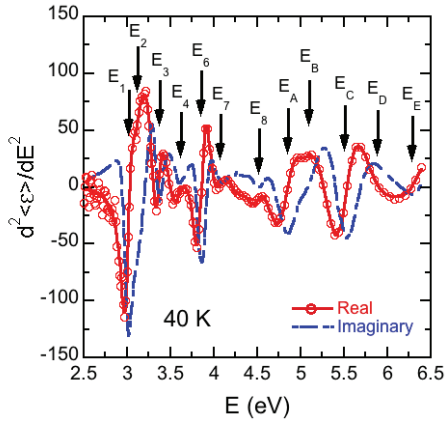
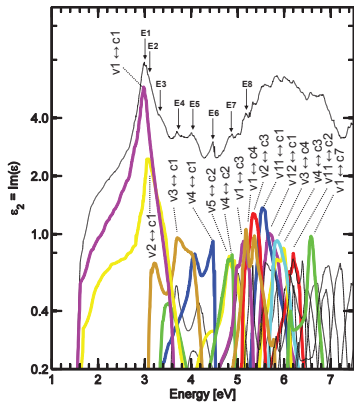
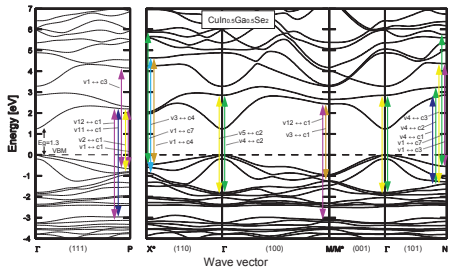


Figure : Energies of each interband critical point (CP) are indicated by arrows and labeled in a numeric and alphabetic order.

# Result 2: Analysis of the imaginary part of dielectric function



**Figure :** Band-to-band analysis of the contribution to the total  $\epsilon_2$  spectrum. The vertical axis is in the log scale.



**Figure :** The calculated electronic band structure of  $\text{Culn}_{0.5}\text{Ga}_{0.5}\text{Se}_2$  where the CPs are identified along the main symmetry directions.

- 1 Background
- 2 Motivation
- 3 Computational methods
- 4 Results
- 5 Summary
- 6 Future perspectives
- 7 Acknowledgements

# Summary

In this licentiate thesis, two major researches are presented:

- Analysis of the electronic structure of  $\text{CuIn}_{1-x}\text{Ga}_x\text{Se}_2$  with  $x = 0, 0.5$ , and 1. Here, we parameterize the energy bands in order to better describe energy dispersions and better analyze the electron and hole dynamics in the materials. We consider intrinsic and *p*-type materials, and we model the temperature dependence.
- Analysis of the optical properties of  $\text{CuIn}_{0.5}\text{Ga}_{0.5}\text{Se}_2$ . Here, the dielectric function spectra is calculated and compared with experimental result. The probable electronic origins of the critical point features are discussed as well.

- 1 Background
- 2 Motivation
- 3 Computational methods
- 4 Results
- 5 Summary
- 6 Future perspectives
- 7 Acknowledgements

# Future perspectives

- The cost and scarcity of indium in the CIGS device is a problem, and copper zinc tin selenide/sulfide (CZT(S,Se)) can therefore be alternative to CIGS due to the low cost and non-toxicity elements.

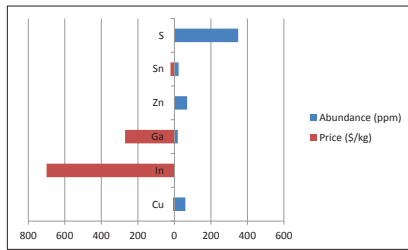


Figure : Abundance and price of Cu, In, Ga, S, Sn, and Zn in Earth's crust (parts per million (ppm) in mass; 10,000 ppm = 1%).

- If there are other similar materials that are of interest. CIGS and CZT(S,Se) can be considered to be in a class denoted as Cu-XY-chalcogenide, where X and Y are two cation elements that replace the group-III In or Ga in CIGS.

1 Background

2 Motivation

3 Computational methods

4 Results

5 Summary

6 Future perspectives

7 Acknowledgements

# Acknowledgements

- I would like to express my sincere appreciation to my supervisor Prof. Clas Persson for his academic encouragement and professional guidance.
- I would like to thank all the group colleagues in Stockholm and Oslo for helpful research discussions and chatting. I would like to thank all other people at the Department of Material Sciences and Engineering at KTH for creating a nice working atmosphere.
- The China Scholarship Council, the Swedish Energy Agency, the Swedish Research Council, Stiftelsen Axel Hultgrens fond, Olle Erikssons stiftelse for materialteknik, and KTH Computational Science and Engineering Centre (KCSE) are acknowledged for financial support.

*Thank you for your attention!*

Rongzhen Chen  
[Rongzhen.Chen@mse.kth.se](mailto:Rongzhen.Chen@mse.kth.se)